BMB Reports - Manuscript Submission

Manuscript Draft

Manuscript Number: BMB-19-234

Title: Inhibition of p90RSK activation sensitizes triple-negative breast cancer cells to cisplatin by inhibiting proliferation, migration and EMT

Article Type: Article

Keywords: Cisplatin; Epithelial-mesenchymal transition; p90RSK; Breast cancer cells; Cell proliferation

Corresponding Author: Kyung-Sun Heo

Authors: Yujin Jin[1], Diem Thi Ngoc Huynh[1], Keon Wook Kang[1], Chang-Seon Myung[1], Kyung-Sun Heo[1,*]

Institution: [1]College of Pharmacy and Institute of Drug Research and Development, Chungnam National University,
[2]College of Pharmacy and Research Institute of Pharmaceutical Sciences, Seoul National University,

Inhibition of p90RSK activation sensitizes triple-negative breast cancer cells to cisplatin by inhibiting proliferation, migration and EMT

Yujin Jin[1], Diem Thi Ngoc Huynh[1], Keon Wook Kang[2], Chang-Seon Myung[1], Kyung-Sun Heo[1*]

[1]College of Pharmacy and Institute of Drug Research and Development, Chungnam National University, Daejeon, South Korea

[2]College of Pharmacy and Research Institute of Pharmaceutical Sciences, Seoul National University, Seoul, 08826, Republic of Korea

Running Title: p90RSK activation in TNBC to cisplatin resistance

Keywords: Cisplatin, Epithelial-mesenchymal transition, p90RSK, Cell proliferation, Breast cancer cells

Corresponding Author's Information:

Kyung-Sun Heo

Tel.: 82-42-821-5927

Fax: 82-42-821-8925

E-mail: kheo@cnu.ac.kr

Abstract

Cisplatin (Cis-DDP) is one of the most widely used anti-cancer drugs. It is applicable to many types of cancer, including lung, bladder, and breast cancer. However, its use is now limited because of drug resistance. p90 ribosomal S6 kinase (p90RSK) is one of the downstream effectors in the extracellular signal-regulated protein kinases 1 and 2 (ERK1/2) pathway and high expression of p90RSK is observed in human breast cancer tissues. Therefore, we investigated the role of p90RSK in the Cis-DDP resistance-related signaling pathway and epithelial-mesenchymal transition (EMT) in breast cancer cells. First, we discovered that MDA-MB-231 cells exhibited more Cis-DDP resistance than other breast cancer cells, including MCF-7 and BT549 cells. Cis-DDP increased p90RSK activation, whereas the inactivation of p90RSK using a small interfering RNA (siRNA) or dominant-negative kinase mutant plasmid overexpression significantly reduced Cis-DDP-induced cell proliferation and migration via the inhibition of matrix metallopeptidase (MMP)2 and MMP9 in MDA-MB-231 cells. In addition, p90RSK activation was involved in EMT via the upregulation of mRNA expression, including that of Snail, Twist, ZEB1, N-cadherin, and vimentin. We also investigated NF-κB, the upstream regulator of EMT markers, and discovered that Cis-DDP treatment led to NF-κB translocation in the nucleus as well as its promoter activity. Our results suggest that targeting p90RSK would be a good strategy to increase Cis-DDP sensitivity in triple-negative breast cancers.

Introduction

Triple-negative breast cancer (TNBC), estrogen receptor (ER)-negative, progesterone receptor (PR)-negative, and human epidermal growth factor receptor (HER2)-negative is a subtype of cancer that exhibits the most aggressive behaviors among breast cancer subtypes (1). The treatment of TNBC is limited because TNBC is insensitive to most hormonal and therapeutic agents. Therefore, TNBC exhibits high recurrence and metastasis with poor prognosis (2). Although various clinical trials, with treatment with cisplatin (Cis-DDP) alone and in combination with other agents have been tested in TNBC, there is still a lack of information on the effect of breast cancer therapy due to drug resistance.

Cis-DDP is an anti-cancer drug that is classified as an alkylating agent. It is widely used in the treatment of ovarian and testicular cancers with a high curative effect and other cancers including small lung, head and neck, and bladder cancers. Cis-DDP exhibits anti-cancer effects via the formation of DNA adducts on inter- and intra-strand cross-links to induce the DNA damage response, cell cycle arrest, and mitochondria-mediated apoptosis. Chemotherapy with Cis-DDP improves the recurrence-free survival rate in women with locally advanced breast cancer (3). However, the development of resistance to Cis-DDP treatment leads to therapeutic failure and tumor recurrence. Therefore, it is important to discover molecular targets to increase the effectiveness of Cis-DDP without drug resistance.

Emerging reports have demonstrated that approximately 70% of TNBC is characterized as basal-like BC. Activated mitogen-activated protein kinase (MAPK) and Akt pathways are involved in TNBCs (4,5). Extracellular signal-related kinase (ERK)1/2 is one of the major MAPK signaling pathways involved in cancer cell proliferation, differentiation, and migration, as well as epithelial-mesenchymal transition (EMT) (5). Various therapies that inhibit MEK-ERK1/2 signaling using a MEK inhibitor (trametinib) or a MEK nucleotide analog (gemcitabine) have been tested in clinical trials with patients who failed multiple therapies (6). However, patients that are treated with MEK inhibitors showed low efficacy with a number of side effects because MEK globally regulates many downstream substrates.

The activation of p90 ribosomal protein S6 kinase (p90RSK), which is a downstream substrate of

ERK1/2 signaling, is associated with tumorigenesis and invasive cancer phenotypes (7). p90RSK contains two functional kinase domains, an N-terminal kinase domain (NTKD) and a C-terminal kinase domain (CTKD) connected by a linker domain (8). Once ERK1/2 is activated by various stimuli, such as carcinogens and growth factors, it can be docked to p90RSK to activate CTKD by phosphorylation of Thr577 (9). Sequential phosphorylation of p90RSK at Thr365 and Ser386 in the linker region induces 3-phosphoinositide-dependent protein kinase-1-mediated NTKD activation that is associated with the activation of p90RSK substrates, including transcription factors, c-Fos, and Myt1 (10). These transcription factors promote cell survival via the regulation of gene transcription, protein synthesis, and the cell cycle (11, 12). However, it has not been revealed whether 90RSK activation is associated with TNBC proliferation and migration via the regulation of transcription factors and the underlying signaling pathway.

In this study, we investigated the role of p90RSK, the downstream effector of the MAPK pathway in the proliferation and migration of Cis-DDP-treated breast cancer cells. We discovered that Cis-DDP treatment increased mRNA expression and protein activation of p90RSK. During the inhibition of p90RSK kinase activation using a p90RSK specific inhibitor, FMK, or a dominant-negative kinase defective mutant, DN-RSK1 transfection significantly decreased cell viability, cell migration, and EMT via the regulation of NF-κB transcriptional activity. Our study aimed to investigate whether the regulation of p90RSK activity is a critical therapeutic target for increasing Cis-DDP sensitivity in patients with TNBC.

Results

Inhibition of p90RSK decreased cell proliferation in MDA-MB-231 cells

Human breast cancer cell lines MDA-MB-231, BT-549, and MCF-7 were treated with 0, 5, 10, and 20 μg/ml of Cis-DDP and cell viability was assessed by the MTT assay. The most significant Cis-DDP-mediated cytotoxicity was shown in MCF-7 cells, whereas MDA-MB-231 and BT-549 cells showed less cytotoxicity after Cis-DDP treatment than MCF-7 cells (Fig 1A). Ki-positive cell data also showed the Cis-DDP resistance in MDA-MB 231 cytotoxicity compared with MCF-7 cells (Fig 1B). As MDA-MB-231 cells presented the strongest Cis-DDP resistance, we determined the cell cycle changes by Cis-DDP in MDA-MB-231 compared with doxorubicin (Dox) treatment. Cis-DDP treatment did not significantly change the G1-S-G2/M cell cycle phase, whereas 5 μg/ml of Dox treatment induced G1 arrest compared with the control sample (Fig 1C). Next, we evaluated p90RSK expression and activation in Cis-DDP-treated cells. The mRNA level of p90RSK was significantly increased by 20 μg/ml of Cis-DDP treatment (Fig 1D). To identify the p90RSK-mediated signaling pathway associated with Cis-DDP resistance in MDA-MB-231 cells, cells were pretreated with a p90RSK specific inhibitor, FMK, for 1 h. FMK treatment only inhibited p90RSK activation, not the phosphorylation of ERK1/2, p38, and Akt (Fig 1E), which showed the specific inhibitory role of FMK on p90RSK activation. It was also investigated whether p90RSK activation and expression in MCF-7 cells were affected by Cis-DDP treatment as in MDA-MB-231, but Cis-DDP treatment did not alter both p90RSK activation and expression in MCF-7 cells (Fig S1A-C). When we examined the inhibitory effect of FMK on p90RSK isoforms, such as RSK1 and RSK2, only the mRNA expression of RSK1 was downregulated by FMK (Fig S2A). Cis-DDP-induced p90RSK activation was completely blocked by FMK pretreatment (Fig 1E). In addition, FMK treatment for 24 h resulted in down-regulation of phosphorylation and protein expression of p90RSK (Fig S2B). FMK treatment and DN-RSK1 transfection-induced inhibition of p90RSK activation significantly sensitized cells to Cis-DDP-induced cell toxicity compared with the control, as shown in Fig 1F and G.

Effect of p90RSK activation on cell migration in Cis-DDP-induced MDA-MB-231 cells

The inhibitory effect of p90RSK activation on MDA-MB-231 cell migration was demonstrated by a scratch wound-healing assay. FMK significantly decreased Cis-DDP-induced migration in MDA-MB-231 cells. Furthermore, the overexpression of dominant-negative p90RSK1 (DN-RSK1) decreased Cis-DDP induced cell migration (Fig 2A and B). Next, we investigated the effect of protein and mRNA expression of matrix metallopeptidase (MMP)2 and MMP9 in migration behavior. Although migrated cells were less visible in cisplatin treatment for 36 hr compared to untreated sample in Fig 2A, both protein and mRNA expression of MMP2 and MMP9 were significantly increased by Cis-DDP treatment for 12 hr (Fig 2C-I). In addition, deactivation and depletion of p90RSK using a FMK treatment and a small interfering RNA (siRNA) completely inhibited Cis-DDP-induced mRNA levels of MMP2 and 9, respectively (Fig 2D-I). Protein expression of p90RSK was depleted by 70% by siRNA of p90RSK compared to siRNA of control (Fig F).

Involvement of p90RSK activation in Cis-DDP-induced EMT

We investigated whether p90RSK regulated EMT on stimulation with Cis-DDP. As shown in Fig 3A–F, mRNA expression of E-cadherin, a tumor repressor, was enhanced in cells treated with Cis-DDP and FMK, whereas mesenchymal markers (N-cadherin and vimentin) and EMT transcription factors (Snail, Twist, and ZEB1) were inhibited in the same condition. To demonstrate the effect of p90RSK activation on Cis-DDP-induced EMT, MDA-MB-231 cells were overexpressed with WT-RSK1 and DN-RSK1 and the mRNA levels of mesenchymal markers and EMT transcription factors were examined. Consistent with the FMK effects shown in Fig 3A–F, DN-RSK1 overexpression, unlike WT-RSK1 overexpression, caused the suppression of EMT by the downregulation of N-cadherin, vimentin, Snail, Twist, and ZEB1 in Cis-DDP-induced cells (Fig 3G–L).

Effect of p90RSK activation on NF-κB transcriptional activity

As we discovered that p90RSK activation is involved in mRNA expression of EMT genes in MDA-

MB-231 cells, we examined NF-κB translocation and transcriptional activity (Fig 4). As shown in Fig 4A and B, Cis-DDP increased NF-κB translocation; however, FMK pretreatment significantly decreased Cis-DDP-induced NF-κB nuclear expression. In addition, Cis-DDP-induced phosphorylation of NF-κB was completely inhibited by FMK treatment (Fig 4C). Next, we investigated the role of p90RSK activation on NF-κB promotor activity. NF-κB promotor activity was strongly increased by 20 μg/ml of Cis-DDP treatment, whereas FMK treatment blocked Cis-DDP-increased NF-κB promotor activity (Fig 4D). TNF-α stimulation was used as a positive control.

Discussion

The purpose of this study was to determine the role of p90RSK activation and its underlying signaling pathway on Cis-DDP drug resistance in breast cancer cells. We evaluated Cis-DDP resistance on cell viability in MDA-MB-231, BT-549, and MCF-7 cells and discovered that in TNBC, MDA-MB-231 exhibited the greatest resistance to cell viability after Cis-DDP treatment. Consistent with the cell viability results, the cell cycle analysis results revealed that 20 μg/ml of Cis-DDP treatment failed to arrest G0/G1, whereas 5 μg/ml of Dox, used as a positive control, strongly arrested G0/G1. We demonstrated the important role of p90RSK activation in Cis-DDP resistance in TNBC. The Cis-DDP treated sample showed both increased protein and mRNA expression of p90RSK in TNBC, MDA-MB-231 cells. This study is the first to show the involvement of p90RSK in Cis-DDP resistance in TNBC.

Recent studies have reported the role of p90RSK in cancer development and progression in various types of cancer (14, 15). p90RSK is a downstream effector of the ERK1/2 signaling pathway and leads to mammalian target of rapamycin complex 1 (mTORC1) activation that results in an increase in BRAF-mutated melanoma cell proliferation *in vitro* (16). p90RSK has also been proposed as an important mediator of cancer cell migration and EMT (17). Furthermore, a recent study showed a high protein expression level of p90RSK in human metastatic breast cancer tissue (7). The depletion of

p90RSK induces the inhibition of CD44 (a tumor-initiating cell phenotype) expression at the cell surface (18). In agreement with previous reports, our data showed that p90RSK phosphorylation was involved in Cis-DDP resistance by inducing cell viability, migration, and EMT. Although a previous report has suggested that the phosphorylation of p90RSK is a potential predictive marker for chemotherapy resistance in ER-positive breast cancer via the Ras/Raf/ERK/p90RSK signaling pathway (19), our results showed that p90RSK expression was higher in TNBC (MDA-MB-231) cells than ER-positive BC (MCF-7) cells. In addition, we demonstrated that MDA-MB-231 cells presented more cis-DDP resistance than MCF-7 cells, with reduced levels of cell viability, proliferation, and G0/G1 arrest.

In figure 1E, we found that FMK treatment inhibited the phosphorylation of p90RSK at Ser380 within 5 min, but not the protein expression of p90RSK. Since we were able to see the changes in the mRNA level of RSK1 by FMK treatment for 24 h, we also tested whether FMK changed protein expression of p90RSK or not. As shown in Fig S2B, Cis-DDP treatment led to an increase in both phosphorylation and protein expression of p90RSK. As the amount of protein expression of p90RSK increases, p90RSK phosphorylation can last for 24 hr. If ubiquitin (Ub) binds to p90RSK and FMK abolishes the Ub binding, FMK-mediated Ub modifications can be altered to p90RSK stability. Therefore, we would like to investigate whether ubiquitination could be involved in protein the stability of p90RSK in the next study.

EMT occurs due to the loss of E-cadherin via many signaling pathways, including the TGF-β signaling pathway and NF-κB signaling pathway (20). We found that p90RSK activation induced NF-κB nuclear translocation and transcriptional activity (Fig 4). Ras-activated MAPK also promotes EMT via the Twist signaling pathway (21). An EMT transcription factor, Twist correlates with MAPK, which is one of the signaling pathways involved in the promotion of breast cancer cell invasion (22). Various transcription factors are related to EMT and cell invasion, and Slug, Snail, and Twist are transcription factors that have been reported to regulate the expression of tumor suppressor such as E-cadherin (23). Our results indicated that p90RSK activation was involved in the upregulation of mesenchymal markers,

such as Snail, Twist, ZEB1, N-cadherin, and Vimentin in Cis-DDP-stimulated MDA-MB-231 cells. The overexpression of WT-RSK1 increased the number of mesenchymal markers induced by Cis-DDP, whereas the inhibition of p90RSK kinase activation reduced the mRNA level of mesenchymal markers and the increased mRNA level of E-cadherin. Since ERK1/2 increases p90RSK activation to stimulate tumorigenesis and invasive cancer phenotypes (5), ERK1/2-mediated p90RSK activation could be involve in NF-κB activation. Many EMT transcription factors including Snail, Twist, and ZEB-1 are activated when NF-κB translocates to the nucleus (13). Therefore, ERK1/2-p90RSK signaling pathway results in NF-κB transactivation-mediated target gene expression, such as Snail, Twist, and ZEB-1.

In conclusion, our study demonstrated, for the first time, that p90RSK kinase was involved in Cis-DDP-mediated cell viability, cell migration, and EMT. Cis-DDP-induced p90RSK activation regulated cell migration via MMP2 and MMP9 expression and EMT via the Snail/Twist/ZEB1 signaling pathway in MDA-MB-231 cells. The inhibition of Cis-DDP-induced p90RSK resulted in the inhibition of NF-κB nuclear translocation and suppressed NF-κB promotor activity. These discoveries reveal a new important mechanism in the research of Cis-DDP resistance in TNBC and that the regulation of p90RSK activity can be a critical therapeutic target for increasing Cis-DDP sensitivity in patients with TNBC.

Materials and methods

Cell culture

Human mammary carcinoma cell lines MDA-MB-231 (HTB-26^{TM}) or MCF-7 (AHTB-22^{TM}) and BT549 (HTB-122^{TM}) were obtained from the American Type Culture Collection (Manassas, VA, USA).

Cell transfection

Rat RSK1 (NM031107) was mutated to K94A/K447A to create a kinase dead protein (DN-p90RSK1) with the QuickChange II site-directed mutagenesis kit (#200521, Agilent) as described previously (24).

Luciferase reporter assay

Cells were transiently co-transfected with pNF-κB-luc and p-TK-renilla reporter plasmid by the DEAE-dextran methods as described previously (25).

Real-Time Polymerase Chain Reaction assay

The quantitative RT-PCR (qRT-PCR) assay was used to analyze the mRNA expression of RSK1, RSK2, MMP2, MMP9, E-cadherin, N-cadherin, vimentin, Snail, Twist, and ZEB1 as described previously (24). The relative gene expression was calculated using a $2^{-\Delta ct}$ method, which was normalized by GAPDH. All primer sequences used in qRT-PCR experiments are listed in Supplementary Table 1.

Statistical analysis

Statistical analysis was performed using GraphPad Prism 5 (version 5.02, GraphPad Software Inc., San Diego, CA, USA). One-way analysis of variance (ANOVA) followed by a Bonferroni multiple comparison was performed. A p value <0.05 was considered significant. All experiments were expressed as the mean ±SEM and were performed independently at least 3 times.

Acknowledgments

This research was supported by Basic Research Lab grant of the National Research Foundation of Korea (NRF) funded by the Ministry of Science, ICT and Future Planning (NRF-2017R1A4A1015860).

Conflict of interest

The authors have no conflict interests.

Figure legends

Figure 1. Inhibition of p90RSK decreases cell proliferation in MDA-MB-231 cells. (A) MDA-MB-231, BT549, and MCF-7 breast cancer cells were stimulated with Cis-DDP for 24 h and cell viability was determined by an MTT assay. (B) Cells were treated with the Cis-DDP for 36 h and cell proliferation was determined by FACS using a Ki-67 proliferation kit. (C) MDA-MB-231 cells were stimulated with 20 μg/ml of Cis-DDP or 5 μg/ml of Dox for 24 h and the cell cycle was investigated using FACS. (D) MDA-MB-231 cells were stimulated with Cis-DDP for 24 h and the protein and mRNA expression of p90RSK were determined by western blotting (upper panel) and qPCR (lower bar graph). (E) MDA-MB-231 cells were stimulated with Cis-DDP for 5 min and whole-cell lysates were subjected to western blot analysis against the indicated antibodies. (F–G) MDA-MB-231 cells were treated with 10 μM of FMK for 3 h (F) or transfected with pcDNA or DN-RSK1 for 18 h (G) followed by treatment with the indicated dose of Cis-DDP for 24 h and cell viability was determined by an MTT assay. The data are presented as means ± SEM (n=3). *p <0.05, **p <0.01 or ***p <0.001 compared with 0 sample; $^{\#}$p <0.05, $^{\#\#}$p <0.01 or $^{\#\#\#}$p <0.001 compared with each control.

Figure 2. Effect of p90RSK activation on cell migration in Cis-DDP-induced MDA-MB-231 cells

(A) Cells were pretreated with 10 μM of FMK for 3 h or transfected with DN-RSK for 18 h followed

by treatment with 20 μg/ml of Cis-DDP. After 36 h, cells were fixed, stained with crystal violet, and photographed using an Olympus microscope. The bar indicates 200 μm. (B) The migration area was measured using Image J software and indicated as fold change compared to the control (0) sample. (C–E) MDA-MB-231 cells were treated with the same conditions as above (Figure 2, A) and whole protein lysates and RNA samples were subjected to western blotting (C) or qPCR (D, E) against MMP2 and MMP9. (F–I) MDA-MB-231 cells were transfected with siRNA from the control (si-Cont) or RSK1 (si-RSK1) for 48 h followed by treatment with 10 or 20 μg/ml of Cis-DDP for 24 h. (F) p90RSK protein expression was determined by western blotting. (G–I) Total RNA samples were subjected to qPCR against RSK1, MMP2, and MMP9 primers. The data are presented as means ± SEM (n=3). *p <0.05, **p <0.01 or ***p <0.001 compared with 0 sample; $^{\#}$p <0.05, $^{\#\#}$p <0.01 or $^{\#\#\#}$p <0.001 compared with each control.

Figure 3. Involvement of p90RSK activation in Cis-DDP-induced EMT. (A–F) MDA-MB-231 cells were pretreated with 10 μM of FMK for 1 h followed by treatment with 20 μg/ml of Cis-DDP for 6 h. (G–L) Cells were transfected with WT-RSK1 or DN-RSK1 plasmids for 18 h followed by treatment with 20 μg/ml of Cis-DDP for 6 h. Total RNA samples were subjected to qPCR against E-cadherin (A and G), N-cadherin (B and H), vimentin (C and I), Snail (D and J), Twist (E and K), and ZEB1 (F and L) primers. The data are presented as means ± SEM (n=3). *p <0.05, **p <0.01 or ***p <0.001 compared with 0 sample; $^{\#}$p <0.05, $^{\#\#}$ p <0.01 or $^{\#\#\#}$ p <0.001 compared with each control.

Figure 4. Effect of p90RSK activation on NF-κB transcriptional activity (A–C) MDA-MB-231 cells were pretreated with 10 μM of FMK for 1 h followed by treatment with 20 μg/ml of Cis-DDP for 1 h. (A) The p65 expression in cells was observed using a laser scanning confocal spectral microscope (Nanoscope systems). Bars indicate 30 μm. (B) Many nuclear p65 NF-κBs were indicated as fold change compared to the control (0) sample. (C) Total protein lysates were subjected to western blotting using anti-phospho or -total p65 antibodies. (D) MDA-MB-231 cells were co-transfected with the pNF-

κB-luc and pRL-Renilla reporter construct. At 18 h after transfection, cells were treated with 10 μM of FMK for 1 h followed by treatment with Cis-DDP or TNF-α (positive control) for 12 h. The luciferase activities of the extracts were determined and normalized based on Renilla luciferase expression. The data are presented as means ± SEM (n=3). ***p <0.001 compared with 0 sample; $^{\#\#}$p <0.01 compared with each control.

Reference

1. Jung J, Jang K, Ju JM, Lee E, Lee JW, Kim HJ, Kim J, Lee SB, Ko BS, Son BH, Lee HJ, Gong G, Ahn SY, Choi JK, Singh SR, Chang S (2018) Novel cancer gene variants and gene fusions of triple-negative breast cancers (TNBCs) reveal their molecular diversity conserved in the patient-derived xenograft (PDX) model. Cancer Lett 428, 127-138

2. Pedersen MH, Hood BL, Ehmsen S, Beck HC, Conrads TP, Bak M, Ditzel HJ, Leth-Larsen R (2019) CYPOR is a novel and independent prognostic biomarker of recurrence-free survival in triple-negative breast cancer patients. Int J Cancer 144, 631-640

3. Dasari S, Tchounwou PB (2014) Cisplatin in cancer therapy: molecular mechanisms of action. Eur J Pharmacol 740, 364-378

4. Verma N, Muller AK, Kothari C, Panayotopoulou E, Kedan A, Selitrennik M, Mills GB, Nguyen LK, Shin S, Karn T, Holtrich U, Lev S (2017) Targeting of PYK2 Synergizes with EGFR Antagonists in Basal-like TNBC and Circumvents HER3-Associated Resistance via the NEDD4-NDRG1 Axis. Cancer Res 77, 86-99

5. Qin H, Liu X, Li F, Miao L, Li T, Xu B, An X, Muth A, Thompson PR, Coonrod SA, Zhang X (2017) PAD1 promotes epithelial-mesenchymal transition and metastasis in triple-negative breast cancer cells by regulating MEK1-ERK1/2-MMP2 signaling. Cancer Lett 409, 30-41

6. Kim HB, Myung SJ (2018) Clinical implications of the Hippo-YAP pathway in multiple cancer contexts. BMB Rep 51, 119-125

7. Ludwik KA, Campbell JP, Li M, Li Y, Sandusky ZM, Pasic L, Sowder ME, Brenin DR, Pietenpol JA, O'Doherty GA, Lannigan DA (2016) Development of a RSK Inhibitor as a Novel Therapy for Triple-Negative Breast Cancer. Mol Cancer Ther 15, 2598-2608

8. Lin L, White SA, Hu K (2019) Role of p90RSK in Kidney and Other Diseases. Int J Mol Sci 20,

9. Chen S, Mackintosh C (2009) Differential regulation of NHE1 phosphorylation and glucose uptake by inhibitors of the ERK pathway and p90RSK in 3T3-L1 adipocytes. Cell Signal 21, 1984-1993

10. Ikuta M, Kornienko M, Byrne N, Reid JC, Mizuarai S, Kotani H, Munshi SK (2007) Crystal

structures of the N-terminal kinase domain of human RSK1 bound to three different ligands: Implications for the design of RSK1 specific inhibitors. Protein Sci 16, 2626-2635

11. Tas I, Han J, Park SY, Yang Y, Zhou R, Gamage CDB, Van Nguyen T, Lee JY, Choi YJ, Yu YH, Moon KS, Kim KK, Ha HH, Kim SK, Hur JS, Kim H (2019) Physciosporin suppresses the proliferation, motility and tumourigenesis of colorectal cancer cells. Phytomedicine 56, 10-20

12. Melhuish TA, Kowalczyk I, Manukyan A, Zhang Y, Shah A, Abounader R, Wotton D (2018) Myt1 and Myt1l transcription factors limit proliferation in GBM cells by repressing YAP1 expression. Biochim Biophys Acta Gene Regul Mech 1861, 983-995

13. Harquail J, LeBlanc N, Landry C, Crapoulet N, Robichaud GA (2018) Pax-5 Inhibits NF-kappaB Activity in Breast Cancer Cells Through IKKepsilon and miRNA-155 Effectors. J Mammary Gland Biol Neoplasia 23, 177-187

14. de Cassia Viu Carrara R, Fontes AM, Abraham KJ, Orellana MD, Haddad SK, Palma PVB, Panepucci RA, Zago MA, Covas DT (2018) Expression differences of genes in the PI3K/AKT, WNT/b-catenin, SHH, NOTCH and MAPK signaling pathways in CD34+ hematopoietic cells obtained from chronic phase patients with chronic myeloid leukemia and from healthy controls. Clin Transl Oncol 20, 542-549

15. Lim W, Yang C, Park S, Bazer FW, Song G (2017) Inhibitory Effects of Quercetin on Progression of Human Choriocarcinoma Cells Are Mediated Through PI3K/AKT and MAPK Signal Transduction Cascades. J Cell Physiol 232, 1428-1440

16. Zhao T, Li R, Tan X, Zhang J, Fan C, Zhao Q, Deng Y, Xu A, Lukong KE, Genth H, Xiang J (2018) Simulated Microgravity Reduces Focal Adhesions and Alters Cytoskeleton and Nuclear Positioning Leading to Enhanced Apoptosis via Suppressing FAK/RhoA-Mediated mTORC1/NF-kappaB and ERK1/2 Pathways. Int J Mol Sci 19,

17. Sheng W, Chen C, Dong M, Wang G, Zhou J, Song H, Li Y, Zhang J, Ding S (2017) Calreticulin promotes EGF-induced EMT in pancreatic cancer cells via Integrin/EGFR-ERK/MAPK signaling pathway. Cell Death Dis 8, e3147

18. Kuwano M, Shibata T, Watari K, Ono M (2019) Oncogenic Y-box binding protein-1 as an effective therapeutic target in drug-resistant cancer. Cancer Sci 110, 1536-1543

19. Moon HG, Yi JK, Kim HS, Lee HY, Lee KM, Yi M, Ahn S, Shin HC, Ju JH, Shin I, Han W, Noh DY (2012) Phosphorylation of p90RSK is associated with increased response to neoadjuvant chemotherapy in ER-positive breast cancer. BMC Cancer 12, 585

20. Ashaie MA, Chowdhury EH (2016) Cadherins: The Superfamily Critically Involved in Breast Cancer. Curr Pharm Des 22, 616-638

21. Wang Y, Zhou BP (2011) Epithelial-mesenchymal transition in breast cancer progression and metastasis. Chin J Cancer 30, 603-611

22. Hong J, Zhou J, Fu J, He T, Qin J, Wang L, Liao L, Xu J (2011) Phosphorylation of serine 68 of Twist1 by MAPKs stabilizes Twist1 protein and promotes breast cancer cell invasiveness. Cancer Res 71, 3980-3990

23. Lin S, Zhang C, Liu F, Ma J, Jia F, Han Z, Xie W, Li X (2019) Actinomycin V Inhibits Migration and Invasion via Suppressing Snail/Slug-Mediated Epithelial-Mesenchymal Transition Progression in Human Breast Cancer MDA-MB-231 Cells In Vitro. Mar Drugs 17, 305

24. Heo KS, Chang E, Takei Y, Le NT, Woo CH, Sullivan MA, Morrell C, Fujiwara K, Abe J (2013) Phosphorylation of protein inhibitor of activated STAT1 (PIAS1) by MAPK-activated protein kinase-2 inhibits endothelial inflammation via increasing both PIAS1 transrepression and SUMO E3 ligase activity. Arterioscler Thromb Vasc Biol 33, 321-329

25. Heo KS, Le NT, Cushman HJ, Giancursio CJ, Chang E, Woo CH, Sullivan MA, Taunton J, Yeh ET, Fujiwara K, Abe J (2015) Disturbed flow-activated p90RSK kinase accelerates atherosclerosis by inhibiting SENP2 function. J Clin Invest 125, 1299-1310

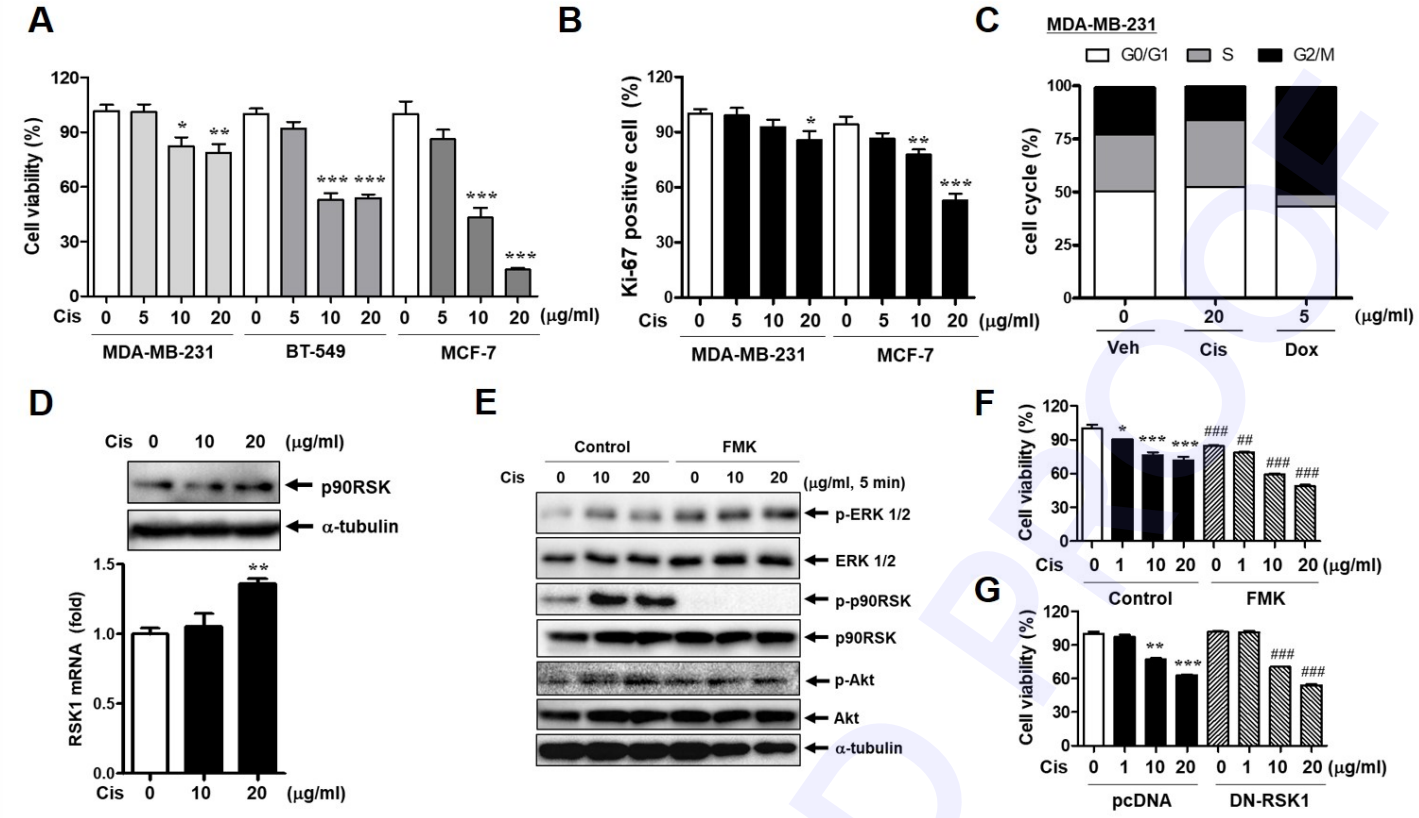

Fig. 1. Figure 1

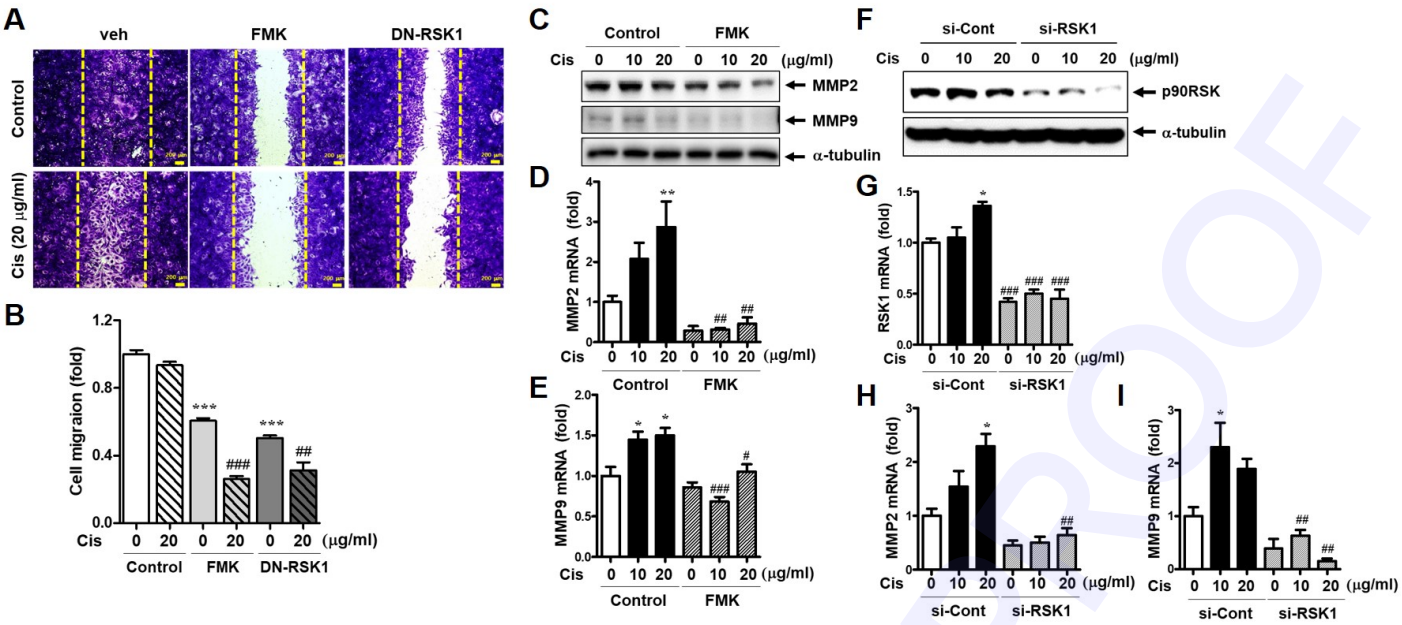

Fig. 2. Figure 2

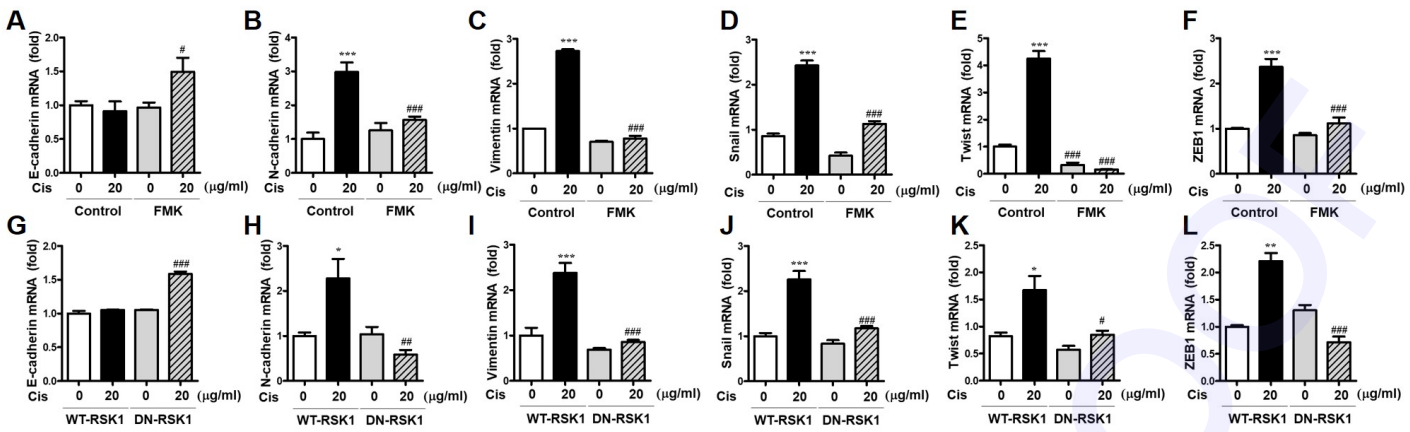

Fig. 3. Figure 3

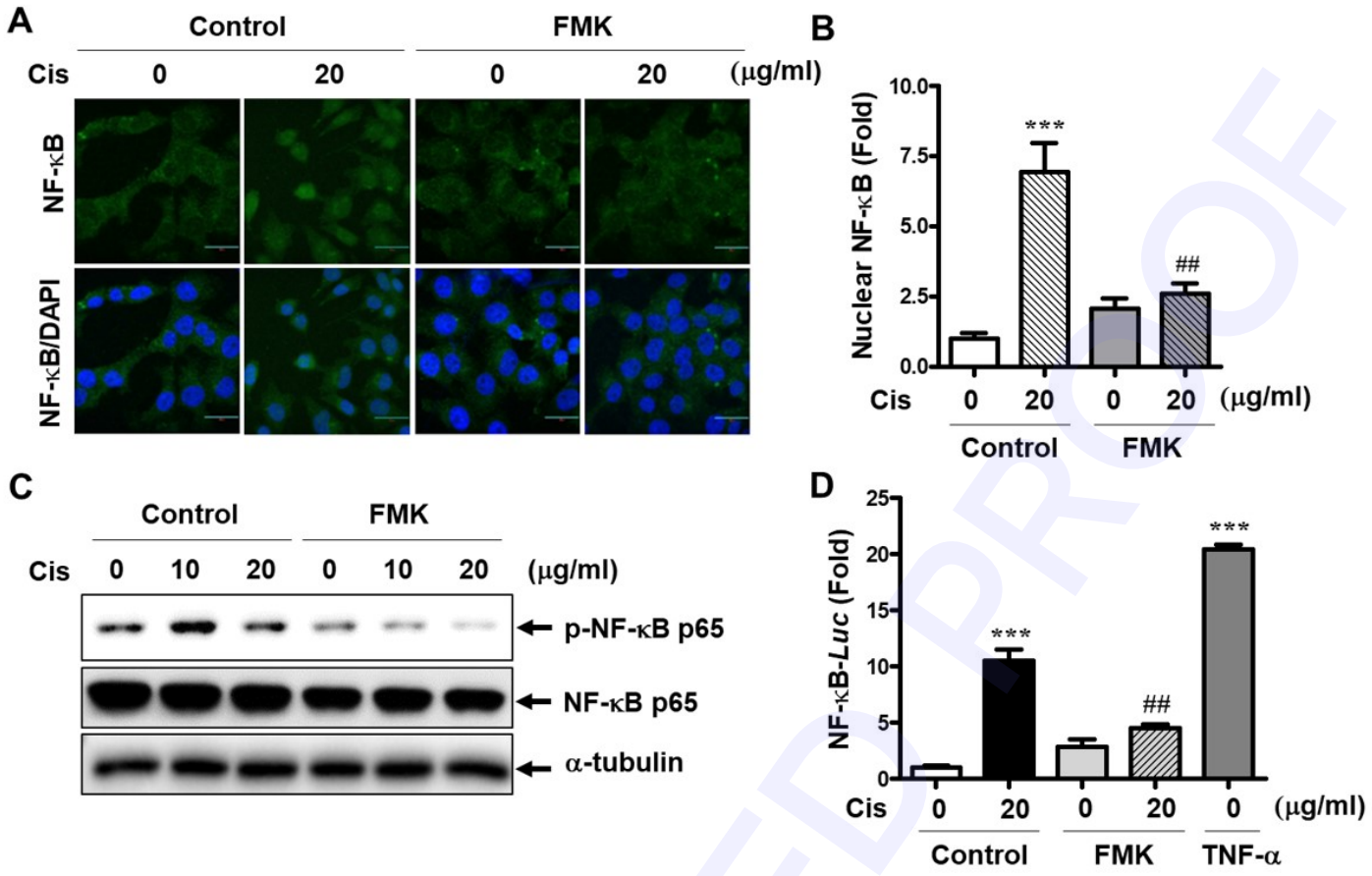

Fig. 4. Figure 4

Inhibition of p90RSK activation sensitizes triple-negative breast cancer cells to cisplatin by inhibiting proliferation, migration and EMT

Yujin Jin[1], Diem Thi Ngoc Huynh[1], Keon Wook Kang[2], Chang-Seon Myung[1], Kyung-Sun Heo[1*]

[1]College of Pharmacy and Institute of Drug Research and Development, Chungnam National University, Daejeon, South Korea

[2]College of Pharmacy and Research Institute of Pharmaceutical Sciences, Seoul National University, Seoul, 08826, Republic of Korea

Running Title: p90RSK activation in TNBC to cisplatin resistance

Keywords: Cisplatin, Epithelial-mesenchymal transition, p90RSK, Cell proliferation, Breast cancer cells

Corresponding Author's Information:

Kyung-Sun Heo

Tel.: 82-42-821-5927

Fax: 82-42-821-8925

E-mail: kheo@cnu.ac.kr

Materials and methods

Reagents and antibody

Rabbit anti-phospho-p38 Thr180/Thr182, rabbit anti-p38, rabbit anti-phospho-Akt Ser473, rabbit anti-Akt, rabbit anti-phospho-NF-κB Ser536, rabbit anti-phospho-p90RSK Ser380, rabbit anti-phospho-ERK1/2, and rabbit anti-ERK1/2 antibodies were purchased from Cell Signaling Technology, Inc. (Danvers, MA, USA). Mouse anti-NF-κB, mouse anti-RSK1, and si-RSK1 were purchased from Santa Cruz Biotechnology (Paso Robles, CA, USA). Rabbit anti-MMP2, rabbit anti-MMP9 antibodies, Muse cell cycle kit (#MCH100106), Muse Ki67 proliferation assay (#MCH100114), and immobilon-P (#IPVH00010) were purchased from Merck millipore. (Burlington, Massachusetts, USA). 10X Phosphate buffered saline (PBS, #EBA-1105) and reveres transcription 5X master mix (#EBT-1511) were purchased from ELPIS-BIOTECH (Daejeon, South Korea). Tri-RNA reagent (#FATRR-001) was purchased from Favorgen (Pingtung, China). DDP (#C2210000), doxorubicin (#D1515), ammonium persulfate (#A3678), 2-mercaptoethanol (#M6250), and skim milk (#70166) were purchased from Sigma-Aldrich (St. Louis, MO, USA). Clarity western ECL substrate (#170-5061), iQ SYBR green supermix (#170-8882AP) were purchased for BIO-RAD (Hércules, CA, USA). EzReprobe (#WSE-7240), EzRIPA Lysis kit (#WSE-7240) were purchased for ATTO corporation (Tokyo, Japan). Dulbecco's modified Eagle's medium (DMEM, #11963-092), RPMI medium 1640 (61870-036), Fetal bovine serum (FBS, #26140-079), Penicillin streptomycin (P/S, #1570-063) and 0.25% Trypsin/EDTA (#25200-072) were purchased from Gibco (Waltham, MA, USA). 3-(4,5-dimethylthiazole-2-yl)-2, 5-diphenyltetrazolium bromide (MTT, #M6494), and Lipofectamine 3000 (#L3000-008) was purchased from Invitrogen (Waltham, MA, USA). EndoFectin™ Max transfection reagent (#EF014) was purchased from GeneCopoeia, Inc (Maryland, USA).

Cell culture and MTT assay

Human mammary carcinoma cell lines MDA-MB-231 (HTB-26^{TM}) or MCF-7 (AHTB-22^{TM}) and BT549 (HTB-122^{TM}) were obtained from the American Type Culture Collection (Manassas, VA, USA). For the cell viability assay, cells were seeded in 96-well at a density of 1 x 10^4 cells per well. After 24

h of stabilization, the cells were treated with various dose of Cis-DDP for 24 h and then cell viability was determined using the MTT assay (Sigma-Aldrich).

Flow cytometry analysis

The Flow cytometry analysis was used to measure cell proliferation and cell cycle using a Muse cell cycle and Ki-67 proliferation kit (#MCH100106 and #MCH100114) according to the manufacture's protocol. Briefly, MDA-MB-231 cells were seeded in 6-well plate at a density of 1 x 10^6 cells/well. For cell proliferation experiment, cells were harvested after 36 h treated with Cis-DDP and fixed for 15 min with a provided fix buffer. Then, cells were permeabilized for 15 min using a provided permeabilization buffer and incubated with an anti-IgG1-PE or an anti-Ki67-PE at room temperature (RT) for 30 min. For cell cycle analysis, cells were harvested after 24 h treated with Cis-DDP and fixed in methanol for 4 h at -20˚C and then incubated in complete media containing Muse cell cycle reagent. The Cell proliferation and the Cell cycle analyses were performed using a Muse cell analyzer (EMD Millipore) and data were analyzed using a MUSE 1.5 analysis program.

Cell transfection

Plasmids including pcDNA and dominant negative (DN)-p90RSK were transfected with EndoFectin™ Max transfection reagent (#EF014, GeneCopoeia) according to the manufacture's protocol. Rat RSK1 (NM031107) was mutated to K94A/K447A to create a kinase dead protein (DN-p90RSK1) with the QuickChange II site-directed mutagenesis kit (#200521, Agilent) as described previously (1).

Luciferase reporter assay

Cells were transiently co-transfected with pNF-κB-luc and p-TK-renilla reporter plasmid by the DEAE-dextran methods as described previously (2). After transfection, cells were treated with 10 μM FMK for 1 h followed by treatment with 20 μg/ml Cis-DDP for 12 h. NF-κB promoter luciferase activity was assayed using a dual-luciferase reporter assay system.

Real-Time Polymerase Chain Reaction assay

The quantitative RT-PCR (qRT-PCR) assay was used to analyze the mRNA expression of RSK1, RSK2,

MMP2, MMP9, E-cadherin, N-cadherin, vimentin, Snail, Twist, and ZEB1 as described previously (1). The relative gene expression was calculated using the $2^{-\Delta ct}$ method, and GAPDH was used for normalization. All primer sequences used in qRT-PCR experiments are listed in Supplementary Table 1.

Supplementary Table 1 – Primer sequence of genes

Genes	Forward primer sequence	Reverse primer sequence
RSK1	TGAAGGTGCTGAAGAAGGCA	CAGCTTCACCACGAATGGGT
RSK2	AACCTATGGGAGAGGAGGAGA	AGGATCTGCCTTTTCATGTCC
Snail	CCCCAATCGGAAGCCTACT	GCTGGAAGGTAAACTCTGGATTAGA
Twist	GGAGTCCGCAGTCTTACGAG	TCTGGAGGACCTGGTAGAGG
ZEB1	GCACCTGAAGAGGACCAGAG	TGCATCTGGTGTTCCATTTT
MMP2	ACAAAGAGTTGGCAGTGCAATA	TCTGGTCAAGATCACCTGTCTG
MMP9	CAGTCCACCCTTGTGCTCTT	CCAGAGATTTCGACTCTCCAC
E-Cadherin	AATTCCTGCCATTCTGGGGA	TCTTCTCCGCCTCCTTCTTC
N-cadherin	TGAGCCTGAAGCCAACCTTA	AGGTCCCCTGGAGTTTTCTG
Vimentin	AGCTAACCAACGACAAAGCC	TCCACTTTGCGTTCAAGGTC
GAPDH	GCACCGTCAAGGGCTGAGAAC	TGGTGAAGACGCCAGTGGA

p90RSK knockdown

To knockdown p90RSK *in vitro*, specific short interference RNA (siRNA) was used (#SC-29475, Santa Cruz Biotechnology). A siRNA that does not match any known human coding cDNA was used as a negative control for silencing (Scramble, sc-37007, Santa Cruz Biotechnology). Transfections were performed using Lipofectamine 3000 (Invitrogen) according to the manufacturer's instructions.

Western blot analysis

Western blotting analysis were performed as described previously (2). Briefly, total protein samples were separated by SDS-PAGE and transferred to nitrocellulose membranes. Western blotting was performed using an each corresponding specific antibody. Polyclonal mouse anti-a-tubulin (Sigma-Aldrich) was used as an internal control.

***In vitro* wound-healing assay**

MDA-MB-231 cells were seeded in 6-well plate at a density of 1 x 10^6 cells/well. After 24 h, the

monolayers were scratched with a 200 μl pipette tip for creating a wound area and washed twice with serum-free media. Cells were treated with FMK or transfected with DN-RSK1 followed by treatment with Cis-DDP for 36 h. The rate of wound closure was assessed and imaged. Each image is derived from the five randomly selected fields.

Immunofluorescent staining

Immunofluorescence assay was performed as described previously (1). Briefly, cells were fixed with 4% paraformaldehyde for 15 min at RT and permeabilized with 0.1% Triton X-100 for 20 min. Cells were incubated with the primary antibodies (p65 1:100) overnight at 4ºC followed by incubation with anti-rabbit secondary antibodies (Invitrogen) conjugated with Alexa 488 at a dilution of 1:400 at RT for 1 h. Cell nuclei were counterstained with 40, 6-diamidino-2-phenylindol (DAPI) for 5 min. Slides were mounted with prolong gold antifade mount reagent (#P36930, Invitrogen) and examined with a laser scanning confocal spectral microscope (Nanoscope systems, South Korea). Representative images were automatically taken using a SPOT digital camera.

Statistical analysis

Statistical analysis was performed using GraphPad Prism 5 (version 5.02, GraphPad Software Inc., San Diego, CA, USA). One-way analysis of variance (ANOVA) followed by a Bonferroni multiple comparison was performed. A p value <0.05 was considered significant. All experiments were expressed as the mean ±SEM and were performed independently at least 3 times.

Supplementary Figures and Figure legends

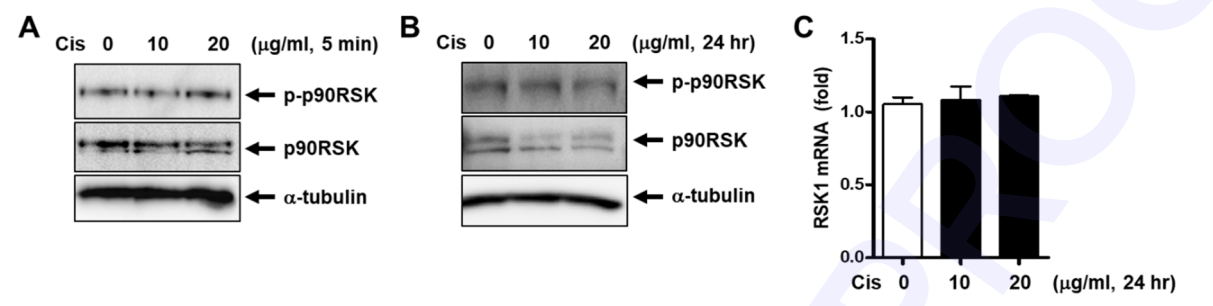

Figure S1

Figure S1. Phosphorylation and protein expression of p90RSK in Cis-DDP-treated MCF-7 cells. (A-B) MCF-7 cell were stimulated with 0, 10, 20 μg/ml of Cis-DDP for 5 min (A) and 24 h (B) and phosphorylation and protein expression of p90RSK were determined by western blotting against indicated antibodies. (C) Messenger RNA level of p90RSK was determined by qPCR against RSK1 primer.

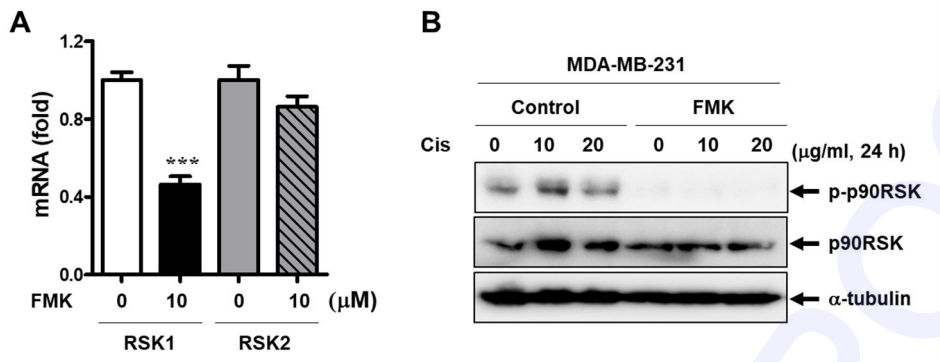

Figure S2

Figure S2. Role of FMK on RSK1 activation and protein expression in MDA-MB-231 cells. (A) MDA-MB-231 cells were treated with 10 μM of FMK for 24 h and total RNAs were subjected to qPCR analysis against RSK1 or RSK2 primers. (B) MDA-MB-231 cells were pretreated with 10 μM FMK for 1 h followed by treatment with 0, 10, 20 μg/ml of Cis-DDP for 24 h. Total protein lysates were subjected by western blotting using anti-phospho or –total p90RSK antibody.

References

1. Heo KS, Chang E, Takei Y, Le NT, Woo CH, Sullivan MA, Morrell C, Fujiwara K, Abe J (2013) Phosphorylation of protein inhibitor of activated STAT1 (PIAS1) by MAPK-activated protein kinase-2 inhibits endothelial inflammation via increasing both PIAS1 transrepression and SUMO E3 ligase activity. Arterioscler Thromb Vasc Biol 33, 321-329

2. Heo KS, Le NT, Cushman HJ, Giancursio CJ, Chang E, Woo CH, Sullivan MA, Taunton J, Yeh ET, Fujiwara K, Abe J (2015) Disturbed flow-activated p90RSK kinase accelerates atherosclerosis by inhibiting SENP2 function. J Clin Invest 125, 1299-1310